ISSN 0016-7029, Geochemistry International, 2024, Vol. 62, No. 11, pp. 1137–1154. © Pleiades Publishing, Ltd., 2024.
Russian Text © The Author(s), 2024, published in Geokhimiya, 2024, Vol. 000, No. 0000, pp. 00000–00000.

Ore Apatite-Bearing Mineralization of the Velimyaki Gabbroid Massif in the Raahe–Ladoga Zone of the Northern Ladoga Region: Identification of Formation Conditions and Estimation of Apatite Age

Sh. K. Baltybaev[a, b, *], R. L. Anisimov[a], I. M. Vasilyeva[a], N. G. Rizvanova[a], O. L. Galankina[a], and V. M. Savatenkov[a, b]

[a] *Institute of Precambrian Geology and Geochronology, Russian Academy of Sciences, St Petersburg, 199034 Russia*
[b] *St. Petersburg State University, Institute of Earth's Sciences, St. Petersburg, 199034 Russia*
**e-mail: shauket@mail.ru*

Received March 12, 2024; revised May 31, 2024; accepted July 23, 2024

Abstract—The Early Proterozoic gabbros of the Velimyaki intrusion of the Northern Ladoga region contain titanomagnetite ore, which has been mined as early as the end of the 19th century. Titanomagnetite horizons are enriched in phosphorus in form of apatite reaching 10 vol %. Isotopic Pb-Pb dating indicates that apatite was likely redeposited during superimposed metamorphism that was significantly separated in time from the magmatic stage of gabbros and clinopyroxene–titanomagnetite ores. Mineralogical, petrological, and isotope-geochemical criteria for the superimposed nature of the mineral formation with apatite recrystallization are the relationship of this mineral with the formation of other metamorphic minerals (hornblende, biotite, sodic plagioclase), the isotopic age of apatite (1790 ± 5 Ma), and the lower temperature (620–710°C) of its formation compared to the crystallization temperatures (900–1260°C) of magmatic minerals. The Pb-Pb age of apatite coincides with the age of metamorphic minerals from other rocks of Late Svecofennian region, as well as with the Rb–Sr ages of biotite and amphibole from host supracrustal rocks. Based on the data obtained, it was concluded that recrystallization of apatite and resetting of the U–Pb system occurred during the Late Svecofennian regional metamorphism.

Keywords: apatite, gabbros, ore, titanomagnetite, metamorphism, Northern Ladoga region, Pb–Pb, Rb–Sr
DOI: 10.1134/S0016702924700654

INTRODUCTION

The accumulation of diverse ore and non-ore mineral resources in the Raahe–Ladoga tectonic zone was facilitated by the favorable tectonic setting in the junction zone of two largest Fennoscandian blocks: Archean Karelian craton and Paleoproterozoic Svecofennian belt (Fig. 1, inset).

The Velimyaki titanomagnetite deposit discovered by Holmberg in 1885 within the eponymous Velimyaki clinopyroxenite–diorite–monzodiorite massif (Ladoga..., 2020) contains titanomagnetite ore bodies in the amphibolized pyroxenite (Gromova, 1951f; *Mineral–Raw Base* ..., 2005), which are mainly confined to the contact of rocks of the first and second phases. Five large lenticular bodies of ore-bearing metapyroxenites were established (Gromova, 1951f). The reserves of titanomagnetite ores are estimated at approximately 130 Mt (*Mineral-Raw Base* ..., 2005), while the predicted vanadium resources are ~100 thousands tons. About 388 thousands tons have been mined by the beginning of 20th century when the deposit exploitation had ceased (*Ladoga* ..., 2020).

In addition to the titanomagnetite ores, the Velimyaki massif contains noble-metal mineralization (Ivashchenko and Lavrov, 1997; Alekseev et al., 2005; Ivashchenko and Golubev, 2011; Alekseev and Kuleshevich, 2017), which together with sulfide dissemination either associates with titanomagnetite ores or occurs in the vicinity of them.

The majority of the deposits and occurrences in the considered region are related to the intrusive rocks, which were studied by many researchers (Saranchina, 1948; *Geological...*, 1970; Lobach-Zhuchenko et al., 1974; Khazov et al., 1993; Bogachev et al., 1999; Baltybaev et al., 2000; Alekseev et al., 2005; *Ladoga...,* 2020, and others). It was noted by most researchers that gabbros of the Velimyaki massif are characterized by the elevated alkalinity, whereas other gabbros of the region define calc-alkaline trends. The elevated alkalinity of the Velimyaki massif is expressed in the appearance of potassium feldspar, the nature of which is controversial. One researchers consider this mineral as magmatic (Saranchina, 1948, 1972), while others (Alekseev et al., 2005) believe that its formation was related to metasomatic processes imposed onto the

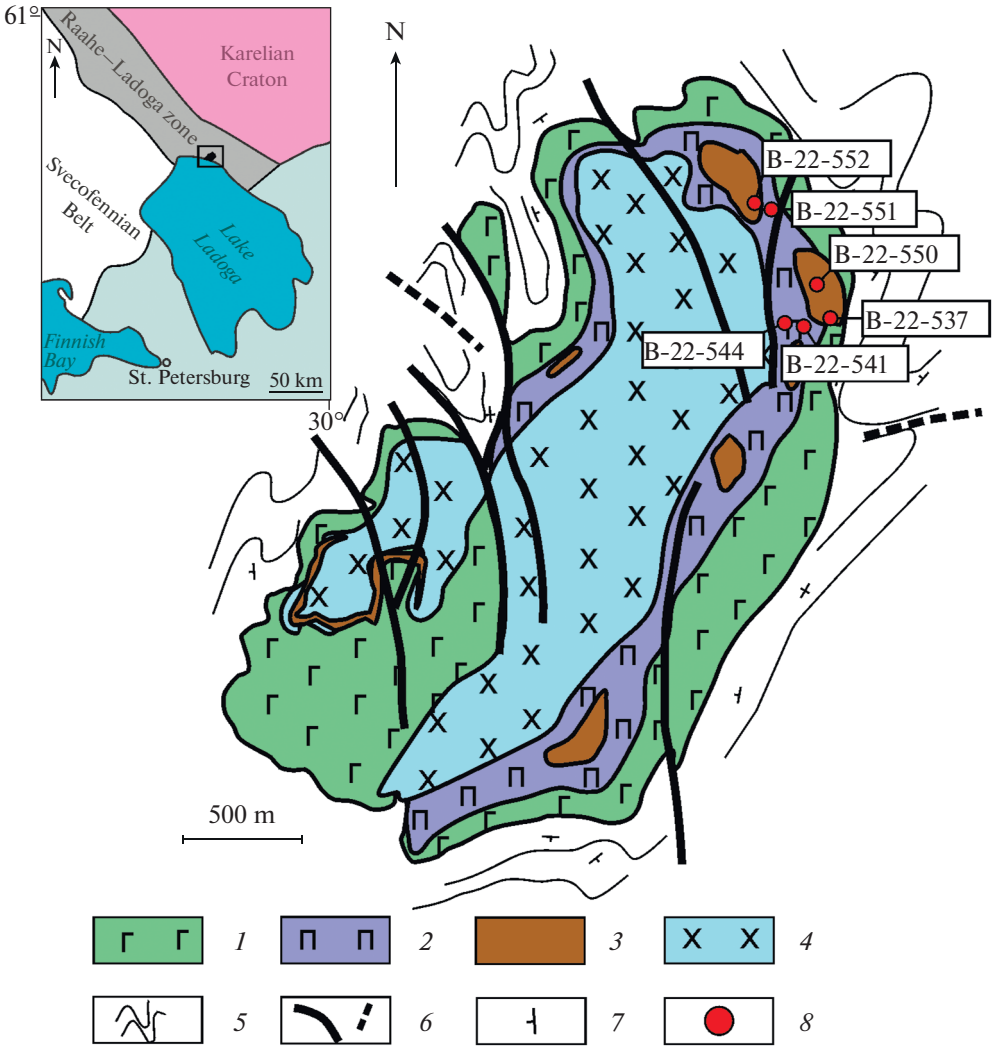

Fig. 1. Tectonic position and schematic geological map of the Velimyaki massif in the Northern Ladoga region. (*1*–*4*) rocks of the Velimyaki massif: (*1*) gabbro (zone of trachytoid gabbro); (*2*) gabbros and diorites with pyroxenite bodies (gabbro–pyroxenite alternation zone); (*3*) ore-bearing clinopyroxenite bodies; (*4*) gabbrodiorites (gabbrodiorite zone); (*5*) host schists of the Ladoga Group; (*6*) faults: proved and inferred; (*7*) dip and strike of foliation; (*8*) sampling localities and numbers. Inset shows the main geological blocks in the southeastern part of the Fennoscandian shield: Early Proterozoic Svecofennian belt, Archean Karelian craton, and Raahe–Ladoga suture between them. Box shows the studied area, where the Velimyaki Massif is located. Simplified schematic map is given after (Alekseev, 2005).

gabbros. An argument in support of postmagmatic alterations of the Velimyaki massif could be the results of U-Pb SIMS zircon isotope dating, which revealed the older age of the gabbros (1894 ± 6 Ma) and younger age of the clinopyroxenites (1874 ± 24 Ma) (*Ladoga*..., 2020). Although these age values agree within error, it is noteworthy that clinopyroxenites (the first phase) gave the younger age compared to the gabbro (second phase). The discordance of age values is likely caused by significant postmagmatic alterations of cliopyroxenites, which, as well be shown below, are expressed also in the appearance of newly formed minerals. These facts in combination with inferred (without evidences) magmatic origin of apatite in the ore association of the clinopyroxenites highlight the need to specify the formation time of apatite in the ores of the Velimyaki massif based on the isotope-geochronological and petrological study.

The characteristic feature of ores of the Velimyaki massif with titanomagnetite mineralization is the coprecipitation of apatite and ore minerals. Apatite, unlike other ore minerals, has high U/Pb ratio and is suitable for U–Pb and Pb–Pb isotope dating of ore crystallization or recrystallization. For this reason, we attempted to study the isotope-geochemical characteristics of apatite and the compositions of associated minerals for estimating the apatite age and thermodynamic parameters of mineral formation. Solution of these questions is of great importance not only for understanding the evolution of rock and ore-forming processes, but also has a decisive practical significance, in particular, in prospecting and exploration works. In

the framework of this work, the main objects were clinopyroxenites of the first phase (and apatite in them), because they host the majority of ilmenite–magnetite ores together with rich apatite mineralization.

METHODS

X-ray fluorescence analysis of the rocks was carried out at the Laboratory of the Karpinsky Institute (St. Petersburg) on an X-ray ARL 9800 spectrometer (Switzerland). Samples were obtained by mixing with a flux (50% lithium metaborate and 50% lithium tetraborate) in proportion 1 : 9, pressed in tablets, and then fused in gold–platinum crucibles. The oxide concentrations were analyzed from 0.01–0.05 wt % depending on the measured component.

The mineral composition was analyzed on a JEOL JSM-6510LA scanning electron microscope equipped with a JEOL JED-2200 energy-dispersive spectrometer at the Institute of Precambrian Geology and Geochronology (St. Petersburg) using complex compounds and pure metals as standards at an accelerating voltage of 20 kV and beam current of 1 nA. Correction for matrix effects was calculated using the JEOL ZAF routine program.

The images of polished thin sections were made using digital photo cameras (10–40X) coupled to a Polam and Olympus optical microscopes and connected with a computer.

The crystallization temperature of minerals was estimated using chemical compositions of minerals and rocks.

The crystallization temperature in the "mineral–melt" system was estimated using equations that describe the linear dependence of equilibrium constants of formation of end members, the components of solid solutions, on the reverse temperature. The equation systems for "olivine–melt", "plagioclase–melt", "magnetite–melt", "ilmenite–melt", and "augite–melt" pairs were taken from a COMAGMAT software package (Ariskin and Barmina, 2000, 2004), which allows one to calculate the compositions of solid phases that are in equilibrium with the melt.

Mineral thermometry was applied for the calculation of formation temperature of minerals of metamorphic stage.

We used the hornblende–plagioclase thermometer by (Holland and Blundy, 1994) based on the equilibrium of calcium amphibole with plagioclase (edenite + albite = richterite + anorthite). The equation of this exchange reaction is suitable for a wide range of amphibole and plagioclase compositions in the quartz-free rocks within the P and T intervals of 1–15 kbar and 400–1100°C, respectively.

The crystallization temperature of biotite was estimated using the (Henry et al., 2005; Wu and Chen, 2015) calibration of Ti-in-biotite thermometer, assuming the chemical equilibrium between postmagmatic minerals containing biotite–ilmenite association. In spite of the fact that Ti-in-*Bt* thermometer was developed for metapelites, we suggest that the geochemical parameters of mineral formation in the studied metabasic rocks at the metamorphic stage were closer to those of felsic rock, which follows from the appearance, in particular, K-feldspar and quartz. Based on the calibration conditions (480–800°C, 3–6 kbar; xMg(*Bt*) = 0.275–1.0, Ti = 0.04–0.6 apfu), the thermometer (Henry et al., 2005) is suitable for the considered rocks. Thermometer (Wu and Chen, 2015) is applicable for the even wider range of temperature and pressure.

The low-temperature transformations of ore minerals were estimated using magnetite–ilmenite thermometer (Lepage, 2003) based on the equation describing the magnetite–ilmenite chemical equilibrium.

The pressure of mineral formation at the metamorphic stage was estimated from Al–Si redistribution in the tetrahedral site of amphiboles and plagioclases using hornblende–plagioclase barometer (Molina et al., 2015), which was calibrated for magmatic and metamorphic rocks in the T and P range of 650–1050°C and 1–15 kbar, respectively.

The U–Pb isotope analysis of minerals was conducted at the Institute of the Precambrian Geology and Geochronology of RAS. To study the U–Pb system of apatites, 5–10 mg aliquots were dissolved in 1N HCl at room temperature for a day. One apatite sample (B-22-552) was subjected to stepwise dissolution. This aliquot was preliminarily washed for 20 min at room temperature in 0.1N HCl, then was successively dissolved in 1N HCl for 10 minutes (L1), 20 minutes (L2), 30 minutes (L3), 40 minutes (L4), and 1 hour (L5). The lead isotope composition was analyzed only in fractions L2, L3, L4, because L1 was likely contaminated by lead of phases related to the later superimposed events, while fraction L5 was contaminated by lead of mineral inclusions in apatite (likely, noncogenetic).

In addition, to determine the isotopic composition of initial lead of apatite, we analyzed plagioclase from plagioclase-bearing rocks. Plagioclase concentrate was extracted in heavy liquids and then hand-picked under the binoculars. Thus obtained plagioclase fraction was ground to powder and sequentially leached in 0.5N HF for 0.5 hour at room temperature and in concentrated (16N) HNO_3 for 4 hours at temperature of 70°C. After that, the sample was kept in acid for 12 hours at room temperature, and then, after solution removal, was treated with concentrated (12N) HCl following the same procedure. Plagioclase was leached to remove the possible radiogenic Pb, which could be accumulated from U-bearing mineral inclusions and iron oxides (on which U could be absorbed). After leaching, the residue was decomposed in a concentrated HF and HNO_3 mixture.

Solutions obtained by the mineral decomposition were divided into two aliquots to determine (1) U and Pb contents; (2) Pb isotopic composition. The U and Pb concentrations were determined by isotope dilution using a mixed spike $^{235}U + {}^{208}Pb$. Lead was extracted on a Bio-Rad® anion-exchange resin in the bromide form following technique (Manhes et al., 1978), while uranium was extracted on a UTEVA SPEC extraction resin in the nitric form. The Pb isotopic composition and Pb and U contents were measured on a Triton TI multicollector mass spectrometer. The Pb and U laboratory blanks were no more than 0.05 and 0.005 ng, respectively. The measured Pb isotopic ratios were corrected for mass fractionation determined as 0.13% per amu by replicate analysis of SRM-982 standard. Processing of initial isotope data and the calculation of isochron parameters were carried out using an ISOPLOT software (Ludwig, 2003). All errors given in tables and used in calculations correspond to 2σ.

The Rb-Sr isotopic analysis of minerals and rocks was conducted at the Institute of Precambrian Geology and Geochronology of the Russian Academy of Sciences. For analysis, the ground monofractions of biotite and amphibole were decomposed in an HF : HNO_3 : $HClO_4$ mixture for 24 hours. The mineral monofractions, except for biotite, were preliminarily treated in 2.2N HCl for 60 minutes to remove the surface pollution and supergene alterations. Prior to the decomposition, the samples were mixed with ^{85}Rb–^{84}Sr spike. After evaporation, the samples were treated with an HCl–HNO_3 mixture for 24 hours. Rb and Sr were extracted on a BioRad® ion exchange resin following technique (Savatenkov et al., 2004). The isotope composition was measured on a Triton TI multicollector solid-source mass spectrometer. The Rb and Sr concentrations and $^{87}Rb/^{86}Sr$ ratios were determined by isotope dilution. The reproducibility of the determination of Rb, Sr concentrations as well as $^{87}Rb/^{86}Sr$ and $^{87}Sr/^{86}Sr$ ratios was calculated by the replicate analyses of BCR-1 standard (6 measurements): [Sr] = 338 (± 0.5%) ppm, [Rb] = 47.5 (±0.6%) ppm, $^{87}Rb/^{86}Sr$ = 0.406 (±0.6%), $^{87}Sr/^{86}Sr$ = 0.705036 (±0.003%). The total blank is 0.05 ng for Rb and 0.2 ng for Sr. The measurements were controlled by the analysis of JNdi-1 and SRM-987 standards. The Sr isotopic composition was normalized to $^{88}Sr/^{86}Sr$ = 8.37521 and adjusted to the certified standard SRM987 $^{87}Sr/^{86}Sr$ = 0.710240. Model ages were calculated in IsoplotR software (Vermeesch, 2018).

BRIEF CHARACTERISTICS OF THE GEOLOGICAL STRUCTURE OF THE MASSIF AND ORE MINERALIZATION IN IT

The Velimyaki massif is an intrusive body differentiated from peridotites and pyroxenites to gabbros and diorite–monzodiorites and has an oval shape 3.5 × 2 km (Fig. 1).

The massif has a heterogeneous structure. It contains numerous small bodies of amphibolized pyroxenites, its central, northern, and northeastern parts are occupied by metamorphosed gabbrodiorites (Saranchina, 1948), while diorites are developed along the western and eastern inner contacts (Alekseev, 2017).

It is suggested that the Velimyaki differentiated massif was formed in several intrusive phases. According to G.M. Saranchina, the rocks were formed in the following sequence: (1) peridotites and pyroxenites, (2) gabbrodiorites, monzonites, and (3) vein rocks of the syenitic series (Saranchina, 1948).

The rocks of the Velimyaki massif were locally cataclased and mylonitized. Along the comparatively small tectonic zones, the rocks were displaced, which disturbed the primary internal structure of the pluton (Saranchina, 1948).

The Velimyaki massif cuts across the schists of the Proterozoic Ladoga Group, as well as underlying amphibolites of the Sortavala group and older Archean granite gneisses. Staurolite–biotite and quartz–biotite schists are developed in the northern and eastern contact, while the southern contact (including the Lake Ladoga coast) is surrounded by schists, amphibolites, and granite gneisses. Surrounding rocks, as significant part of the massif, bear signs of epidote—amphibolite and amphibolite metamorphic facies. According to isotope dating of rocks and minerals, the regional polychronous metamorphism occurred within 1.87–1.79 Ga (Baltybaev et al., 2005, 2009: *Ladoga...,* 2020).

The isotopic U–Pb (SIMS) age of the Velimyaki intrusion was determined on zircons from leucogabbro, the concordant age of which is 1894 ± 6 Ma (Alekseev et al., 2005; Alekseev and Kuleshevich, 2017).

Ore mineralization in the Velimyaki massif is confined to the pyroxenite bodies. Two types of mineralization are distinguished: (1) titanomagnetite mineralization with the elevated concentrations of vanadium and elevated apatite content; (2) noble-metal sulfide mineralization.

The titanomagnetite mineralization is represented by the disseminated and schlieren ore segregations, the volume of which in high-grade ores reaches 10–40%. Sporadic massive ores contain up to 90% titanomagnetite. These ores are dominated by titanomagnetite, while ilmenite is the second in abundance. The ilmenite and titanomagnetite have the elevated content of V_2O_5 (up to 2 wt %). The apatite content is 3–10 vol %.

The noble metal mineralization is confined to the sulfide dissemination and/or veinlets consisting of pyrite–chalcopyrite or chalcopyrite–pyrite–pyrrhotite association. The insignificant amount of native Au is confined to the disseminated–vein sulfide ores. There is also pyrite mineralization, which is later than pyrite–chalcopyrite one.

Rich sulfide mineralization is usually confined to the zones of fracturing and hydrothermal–metasomatic reworking. The thickness of the sulfide veins

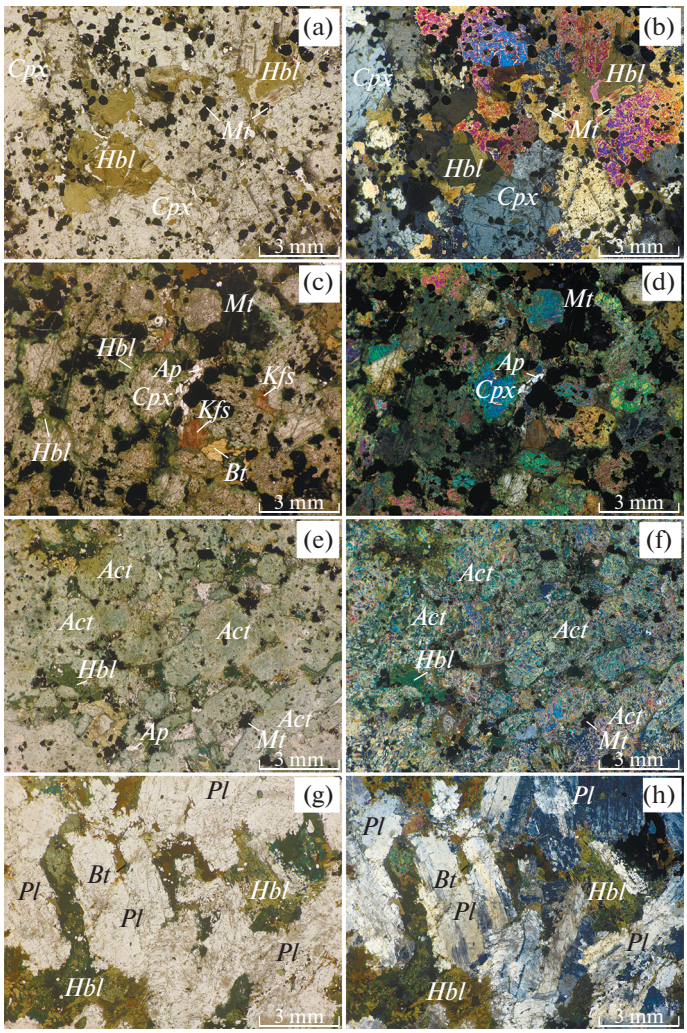

Fig. 2. Photos of polished thin sections of main rock types of the Velimyaki massif. (a–f): variably metamorphosed pyroxenites of the first phase: unaltered (sample B-22-537-1 (a, b), weakly altered, sample B-22-550 (c, d), highly altered – sample B-22-552 (e, f); (g, h): diorites of the second phase – sample B-22-541. Images are made under parallel (a, c, e, g,) and crossed (b, d, f, h) nicols. Hereinafter, mineral abbreviations are given according to (Whitney and Evans, 2010).

accounts for from 15–20 cm to 40 cm in swells, while a length of 1.5–2 m (*Ladoga...*, 2020). In the ore zones, the mineral formation occurred in several stages: the biotite–amphibole association is overprinted by quartz–feldspathic and carbonate parageneses with tourmaline, biotite, epidote, chlorite, and microcline. Accessory minerals in the ores are represented by sphalerite, pentlandite, galena, molybdenite, cobaltite, arsenopyrite, and more rare hessite, tellurobismuthite, stuetzite, and tetradymite.

The noble-metal mineralization in the Velimyaki massif is ascribed to the low-sulfide Pt–Pd type with total Pt, Pd, Au content up to 0.7 ppm (*Ladoga ...,* 2020).

PETROGRAPHY AND MINERALOGY

The petrographic features (Fig. 2) and qualitative composition of minerals from rocks of the first and second phases are mainly determined by the degree of postmagmatic alterations of the rocks and indicate a heterogeneous manifestation of regional metamorphism and fluid–thermal influence along the local tectonic zones.

Petrographic Characteristics of Rocks of the First and Second Phases of the Velimyaki Massif

The rocks of the first phase are mainly pyroxenites. Their petrographic features are characterized below, with subdivision of rocks based on the metamorphic grade.

Unmetamorphosed pyroxenites (samples B-22-537- and, B-22-537-2) consist of clinopyroxene (50–70 vol %), brownish, supposedly magmatic hornblende (7–40 vol %), and ore minerals represented by magnetite and ilmenite (7–20 vol %). Subordinate minerals are represented by mafic mica (phlogopite) and chlorite. Microtexture of the rocks is hypidiomorphic.

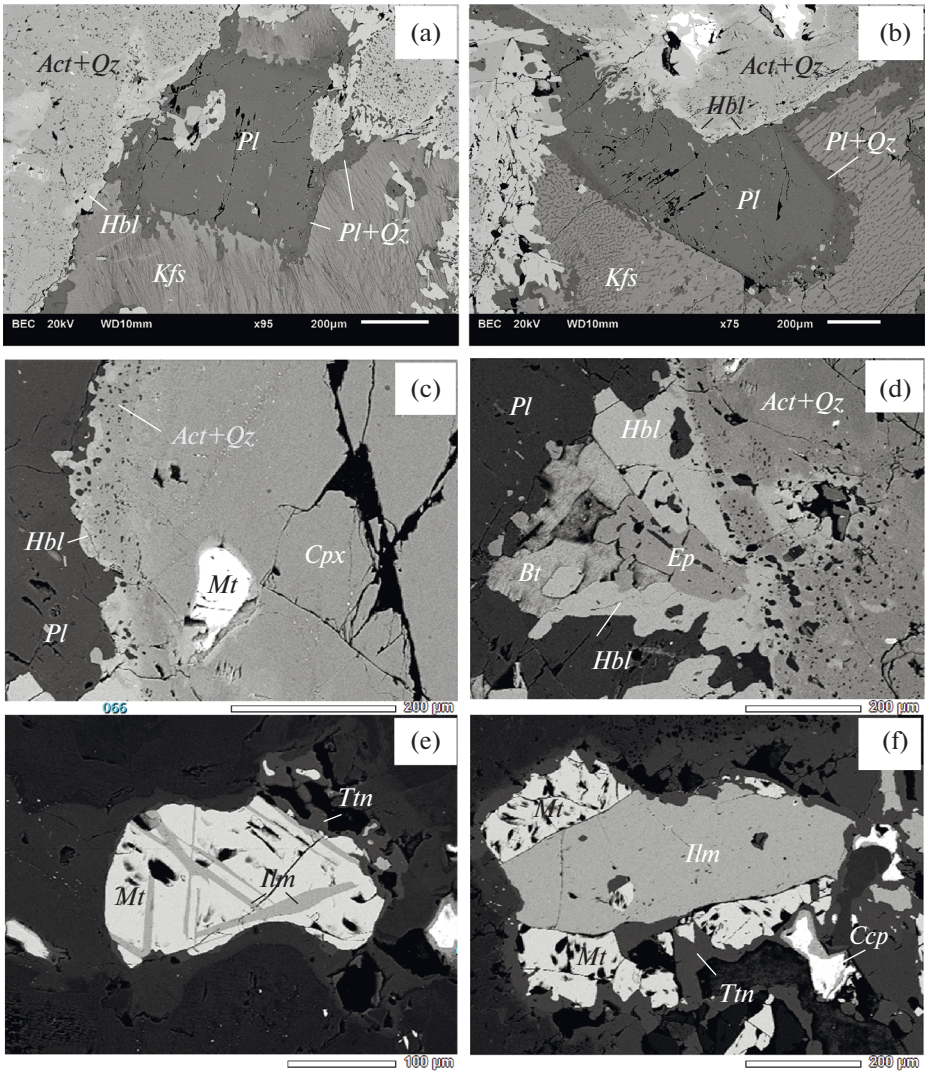

Fig. 3. BSE images of recrystallized minerals from the monzogabbro of the Velimyaki massif (sample B-22-552-1). (a, b) reaction relations of K-feldspar and plagioclase; (c, d) hornblende (sometimes with biotite and epidote) rims around actinolite pseudomorphs after clinopyroxene; (e, f) magnetite grains with exsolution lamella made up of ilmenite; the grain is surrounded by titanite.

The clinopyroxene forms colorless hypidiomorphic round or elongate grains. The hornblende is represented by xenomorphic grains filling interstices between clinopyroxene crystals, but also occurs as small xenomorphic inclusions in clinopyroxene. The rock also contains fine ore dissemination likely represented by ilmenite. Magnetite forms round grains without visible crystallographic outlines, which are confined to the aggregates of clinopyroxene crystals. Ilmenite forms drop-like segregations in magnetite crystals or exsolution lammelae (Fig. 3).

Weakly and highly metamorphosed pyroxenites and monzogabbros that preserved magmatic texture (samples B-22-550, B-22-552, and B-22-552-1). The rocks are composed of clinopyroxene up to 40 vol % in weakly altered varieties (B-22-550) to its complete absence in the highly altered rocks (B-22-552), magnetite and ilmenite (0–25 vol %), K-feldspar and plagioclase (in total from a few percents in pyroxenites (B-22-550) to 50 vol % in the monzogabbro (B-22-552-1)), and apatite (up to 3 vol %). Secondary minerals are represented by actinolite (up to 70 vol % in the highly altered varieties, for instance in B-22-552), hornblende (around 20 vol %), and biotite (1–20 vol %). The rocks have blastohypidiomorphic microtexture.

The manifestations of clinopyroxene, magnetite, and ilmenite are similar to those of the unaltered pyroxenites. The grains of ore minerals could be surrounded by titanite rim (Fig. 3). The K-feldspar forms xenomorphic grains, fills interstices between clinopyroxene grains. The microcline lattice and perthites are also observed. Significant amounts of plagioclase are observed only in monzogabbro (B-22-552-1) and form euhedral crystals. Myrmekites are observed at

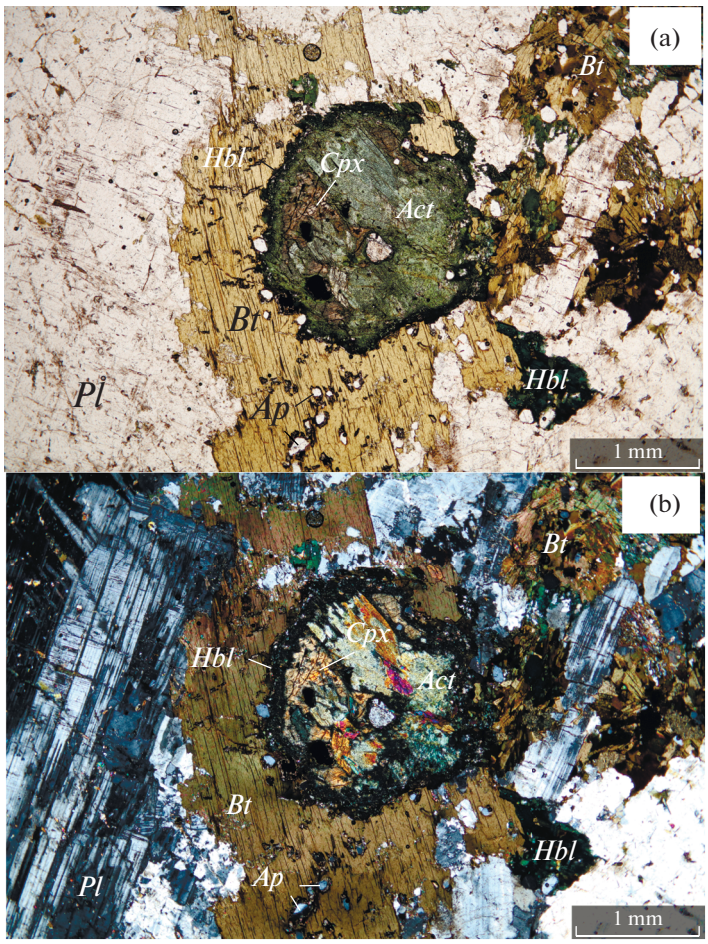

Fig. 4. Photos of polished thin section of monzodiorite in the parallel (a) and crossed (b) nicols, which show a successive replacement of magmatic clinopyroxene by actinolite (± quartz) aggregate and development of hornblende after actinolite. Apatite grain frequently occurs in association with hornblende and secondary biotite.

the contact with K-feldspar (Fig. 3). Amphiboles in the altered pyroxenites are represented by brown hornblende, green hornblende, and actinolite. The brown hornblende is likely magmatic, similar to that described in the unaltered pyroxenites. It forms small grains within clinopyroxene crystals. The green hornblende and actinolite are developed after clinopyroxene.

In the weakly altered pyroxenite (B-22-550), the green hornblende replaces clinopyroxene along grain boundaries. The highly altered rocks (B-22-552, B-22-552-1) contain pseudomorphs after clinopyroxene grains (Figs. 3, 4), where pseudomorph centers are made up of actinolite aggregates, while rims, of the green hornblende. The pseudomorphs could retain clinopyroxene relicts (sample B-22-552-1), but complete recrystallization is also observed (B-22-552). Biotite forms xenomorphic grains that are spatially confined to the magnetite grains. Apatite forms single hypidiomorphic crystals, more rarely, accumulations of grains. Its crystals have elongate-prismatic shape; polished thin sections are dominated by cross-sections perpendicular to the elongation axis. Apatite mainly occurs in the interstices between clinopyroxene grains, where it associates with hornblende.

Highly metamorphosed pyroxenites that lost magmatic texture (sample B-22-551). They are made up of biotite (40 vol %), amphibole (40 vol %), carbonate (10 vol %), magnetite and ilmenite (5 vol %), and apatite (1 vol %). The rocks have a nematolepidoblastic microtexture with cataclastic elements. The biotite occurs as large pale yellow to brown crystals. The crystals are deformed, bent, and locally recrystallized into a fine flaky aggregate. The amphiboles compose aggregates of hypidiomorphic or xenomorphic crystals of hornblende and actinolite. The carbonate forms lenticular segregations within biotite, as well as separate grains of irregular shape. The morphologies of magnetite and ilmenite are similar to those described above; sometimes, titanite rims are developed around ore minerals. Apatite was found as accumulation of single euhedral crystals.

The rocks of the second phase are diorites and monzodiorites (samples B-22-541 and B-22-544). They are composed of plagioclase (50–80 vol %), amphi-

bole–-hornblende and actinolite (10–20 vol %), biotite (10–20 vol %), apatite (5 vol %), and ore mineral (1 vol %). Clinopyroxene relicts are also observed. The rocks have blastogabbroophitic microtexture. Plagioclase forms large hypidiomorphic lath-like crystals. The crystals are deformed into bent twins and fractured. The grain margins are granulated. In the least altered rocks (B-22-544), amphiboles form pseudomorphs after clinopyroxene, which are similar to those described in pyroxenites. Thereby, some pseudomorphs retain actinolite cores and hornblende rims, while in some cases, actinolite is replaced by an aggregate of hornblende and quartz. In such pseudomorphs, hornblende could associate with biotite. In the more altered rocks (B-22-541), pseudomorphs are not preserved and give way to the intergrowths of hypidiomorphic or xenomorphic crystals of hornblende and biotite, while a hornblende–quartz aggregate is sometimes preserved in the central parts. Biotite occurs in the intergrowths with hornblende or forms separate large xenomorphic crystals. Apatite is observed as separate hypidiomorphic crystals, which are usually confined to the hornblende–biotite intergrowths.

Thus, the petrographic features of the studied rocks indicate the presence of mineral associations that are ascribed to the different stages of mineral formation: magmatic and postmagmatic–metamorphic ones.

The metamorphic transformations of the rocks are characterized by the simultaneous growth of plagioclase, amphibole, and biotite. Actinolite frequently replaces early clinopyroxene in its rims or forms complete pseudomorphs. In the last case, some amount of quartz is formed together with the actinolite. A noteworthy and important feature of this superimposed actinolite is its subsequent replacement by dark green hornblende. The newly formed mineral assemblage represented by hornblende (hastingsite and Fe-rich ferrihornblende) and plagioclase is observed practically in all polished thin sections of altered clinopyroxenites or gabbros (Figs. 2, 4). Locally, the content of this assemblage reaches 30 vol %. The above described hornblende associates with secondary brown biotite. Its content in the rock reaches 5–8 vol %. Biotite grains as intergrowths with hornblende are developed after clinopyroxene or actinolite.

Host rocks. At the modern erosion surface, the gabbros of the Velimyaki massif have direct intrusive contacts with the Early Proterozoic amphibolites of the Sortavala Group and biotite–garnet, biotite, two-mica gneisses, as well as diverse andalusite-, sillimanite-, and staurolite-bearing schists of the Ladoga Group (*Ladoga ...,* 2020).

The studied amphibolites consist mainly of hornblende (70–90 vol %), plagioclase (10–20 vol %), and sometimes contain quartz, biotite, and accessory amounts of magnetite, ilmenite, and titanite. Secondary minerals are represented by chlorite, higher-Fe biotite, and actinolite. The rock has a nematogranoblastic, coarse-grained texture and massive, locally schistose structure.

Two-mica gneisses consist of biotite (20–25 vol %), muscovite (5–10 vol %), plagioclase (30–35 vol %), quartz (20–30 vol %), and opaque minerals (1–2 vol %). The texture is medium-grained lepidogranoblastic, and structure is gneissose, banded. The garnet–biotite gneiss studied by Rb-Sr method consists of biotite (20–25 vol %), garnet (up to 20 vol %), plagioclase (up to 30 vol %), quartz (20–25 vol %), and opaque minerals (1–2 vol %). The rock has medium-grained lepidogranoblastic texture and gneissose, banded structure.

The Mineralogy of Rocks of the First and Second Phases of the Velimyaki Massif

Selected chemical compositions of minerals of the Velimyaki massif are given in the Supplementary EMS1_tabl_minerals.

Clinopyroxenes in the rocks of the first phase are represented by diopside and augite (XMg = 0.69–0.87). In the second phase, clinopyroxene is rarely preserved as relicts in the hornblende–actinolite pseudomorphs. It is represented by augite of slightly higher Fe composition (XMg = 0.60–0.66) than clinopyroxene from the rocks of the first phase.

Brownish **amphiboles** are supposedly magmatic, occur in some pyroxenites of the first phase (samples B-22-537-2 and B-22-550), and are represented by magnesiohastingsite and Ti-bearing magnesiohastingsite. In the rocks of the first phase, green hornblendes form rims around pseudomorphs after clinopyroxene and are mainly represented by potassic hastingsite, hastingsite, and Fe-rich ferrihornblende. The central parts of the pseudomorphs are made up of actinolite and, to lesser extent, of magnesio-ferrihornblende.

In the rocks of the second phase, the hornblendes form both rims in the hornblende–actinolite pseudomorphs and separate intergrowths (Figs. 3, 5). They are represented by the Fe-rich ferrihornblende, potassic hastingsite, and Fe-rich ferritschermackite. The central parts of the pseudomorphs are composed, as the rocks of the first phase, of actinolite and magnesio-ferrihornblende.

Amphiboles that compose rims around pseudomorphs are much higher Fe (on average, XMg = 0.38) than amphiboles from the central parts (on average, XMg = 0.59). For comparison, XMg(av.) of brown hornblende is 0.70.

Amphiboles of the massif are characterized by the potassium admixture, the highest content of which is observed in the Fe-rich amphiboles that compose pseudomorph rims (K_2O content in them is 1.5 wt %). These amphiboles also have a ubiquitous admixture of chlorine (on average, 0.28 wt %).

The compositional features of the amphiboles from rocks of two phases of the Velimyaki massif are shown in Fig. 5.

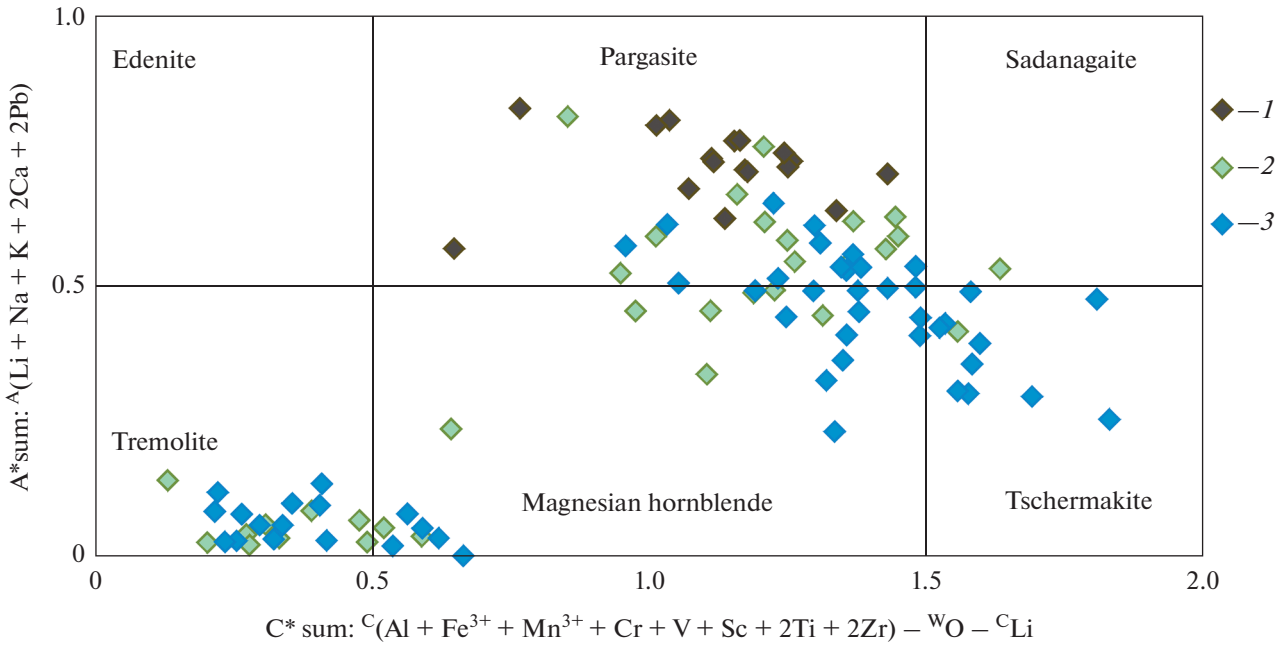

Fig. 5. Amphiboles from rocks of the first and second phases of the Velimyaki massif. (*1*) compositions of supposedly magmatic amphiboles of the rocks of the first phase, (*2*) compositions of metamorphic amphiboles in transformed rocks of the first phase, (*3*) compositions of metamorphic amphiboles in transformed rocks of the second phase. Diagram and calculations of amphibole composition are after (Locock, 2014).

Biotite in both phases have similar compositions and are represented by phlogopite– annite (XMg = 0.34–0.61). The aluminum content in tetrahedral site varies from 1.1 to 1.3 a.p.f.u. The mineral usually contains titanium admixture amounting 1.4–2.7 wt % and also insignificant admixture of chlorine (up to 0.29 wt %).

Plagioclase in the rocks of the first phase is present in the most silicic derivatives (monzogabbro, sample B-22-552-1). It is represented by andesine–oligoclase An40–13. In the rocks of the second phase, plagioclase is one of the rock-forming minerals. In the monzodiorite (sample B-22-544), it forms large zoned crystals, which consist of labradorite (An55) core gradually changing into oligoclase An19 rim. In the diorite (sample B-22-541), plagioclase is composed of labradorite–andesine (An56–44) core and thin rims represented by andesine–oligoclase An35–20. The cores likely have a magmatic nature, while rims are metamorphic in origin. In such case, the essentially sodium compositions of plagioclase could indicate their late metamorphic nature.

Magnetite in the studied rocks occurs both in intergrowths with ilmenite and as separate crystals. It is characterized by a ubiquitous admixture of V_2O_5 (1.27–2.74, averaging 0.52 wt %). In addition, the mineral contains insignificant admixture of SiO_2 (0–0.64 wt %), TiO_2 (0–0.60 wt %), and Al_2O_3 (0–0.91 wt %). Sometimes, it contains trace chromium (0.24–0.53 wt %).

Ilmenite was found in all studied rocks and frequently associates with magnetite. It practically always contains admixtures of MnO (2.06–3.76 wt %) and MgO (0.13–0.75 wt %). Other admixtures are not typical, except for the scarce insignificant admixture of Cr_2O_3 (0.19 wt %).

Apatite forms euhedral grains 0.01–0.2 mm in size in amphibole, biotite, and, more rarely, in plagioclase and clinopyroxene. It is represented by the fluorapatite–hydroxyl-apatite series (Fig. 6) and could contain insignificant admixture of chlorine (up to 0.36 wt %).

RESULTS OF ISOTOPE ANALYSIS OF APATITE AND THERMOBAROMETRY OF THE ROCKS

Pb–Pb age of apatite

Apatites extracted from clinopyroxenite samples (Fig. 7, Table 1) yields an age range from 1737 to 1801 Ma with a maximum error of ±7 Ma.

Presented age values were calculated from two-point isochrons, which can be interpreted only as approximate age of apatite. In addition, the content of plagioclase in the clinopyroxenites is too low to extract this mineral in amounts sufficient for Pb isotope analysis. For this reason, data on the initial Pb isotope composition of pyroxenites are estimated indirectly from the initial lead isotopic composition of plagioclase from monzogabbro. Thus, it is more reliable to plot Pb–Pb isochron using composition points of fractions of stepwise dissolution of apatite from clinopyroxenite and, supposedly cogenetic plagioclase extracted from more felsic varieties (sampled from the

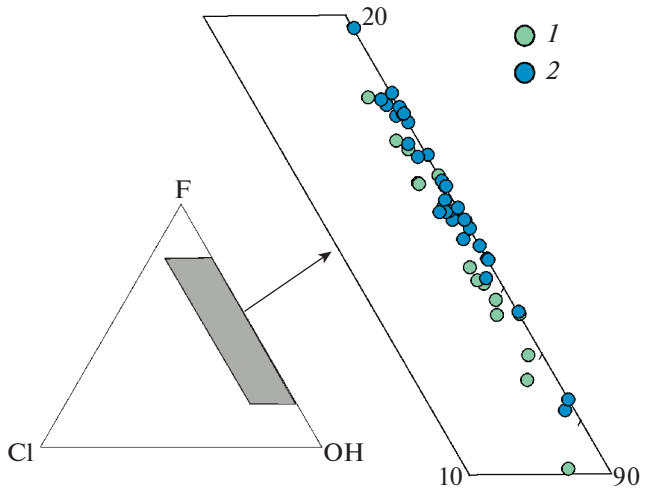

Fig. 6. Content of volatile components in the apatites from rocks of the first and second phases of the Velimyaki massif. (*1*) apatites from rocks of the first phase, (*2*) from rocks of the second phase.

same exposure). Thus, to construct the $^{206}Pb/^{204}Pb$–$^{207}Pb/^{204}Pb$ diagram, we used lead isotopic compositions of intermediate leachates obtained by stepwise dissolution of apatite monofraction (Fig. 8a). The first and last leachates (L1 and L5) were not used for the measurements as probably containing the alien lead from surface admixtures (L1) or microinclusions in apatite (L5). Using such methodical approach, Pb-Pb isotopic age of apatite from pyroxenite was determined as 1790 ± 5 Ma (MSWD = 0.14), which is consistent with preliminary age estimates of apatite from other pyroxenite samples on two-point isochrons presented above (Fig. 7).

For sample B-22-522-1, which in composition corresponds to the monzogabbro, two-point Pb–Pb isochron was constructed using Pb isotopic compositions of apatite and plagioclase extracted from this sample (Fig. 8b, Table 2). The isochron defined by Pb isotopic compositions of prismatic well-shaped apatites and supposedly magmatic plagioclase define an age of 1842 ± 10 Ma.

Age estimates obtained at stepwise dissolution of apatite correspond to Rb-Sr model age of micas and amphiboles from rocks that host metagabbroids (Table 2).

Thermobarometry of the Rocks

The mineral composition of the studied rocks provides insight into the temperature regime of their formation at the magmatic and metamorphic stages.

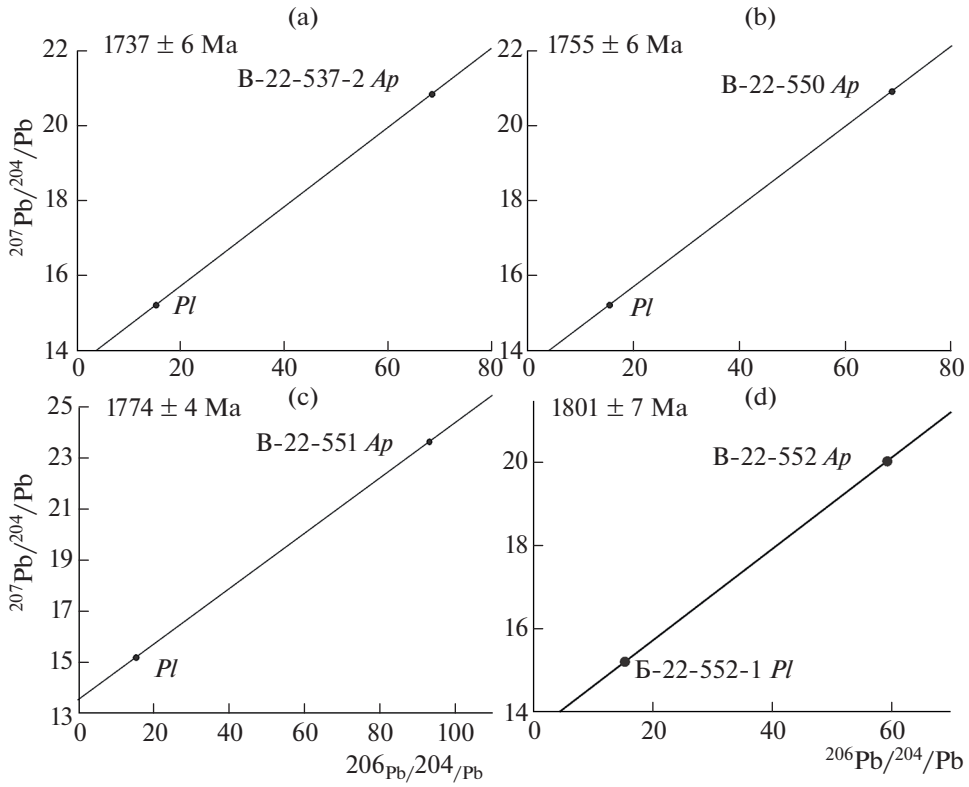

Fig. 7. Two-point Pb–Pb isochrons for apatites from the first phase of the Velimyaki massif. (a) unmetamorphosed clinopyroxene (sample B-22-537-2), (b) weakly metamorphosed pyroxenite (sample B-22-550), (c) highly metamorphosed pyroxenite (sample B-22-551), (d) pyroxenite (B-22-552). Isotope composition of plagioclase from the most felsic derivatives of the first phase was used. In all diagrams, one isotope composition of plagioclase from most felsic derivatives of the first phase was used (sample B-22-551-1).

Table 1. U–Pb isotope analysis of apatite and plagioclase from rocks of the Velimyaki massif

Ordinal no.	Sample number, fraction, mineral	Pb, ppm	U, ppm	$^{238}U/^{204}Pb$	$^{206}Pb/^{204}Pb$	$^{207}Pb/^{204}Pb$	$^{208}Pb/^{204}Pb$
1	B-22-537-2, *Ap*	4.73	6.15	165.3	68.505	20.854	56.898
2	B-22-550, *Ap*	11.4	14.1	164.6	68.640	20.923	63.808
3	B-22-551, *Ap*	9.51	13.2	234.6	93.238	23.651	78.096
4	B-22-552. *Ap*	10.9	11.4	128.1	59.310	20.043	60.994
5	B-22-552 20′ 1N HCL	78 ng	94 ng	167.3	71.151	21.308	67.590
6	B-22-552 30′ 1N HCL	79 ng	96 ng	169.8	71.604	21.360	67.296
7	Б-22-552 40′ 1N HCL	63 ng	75 mg	161.8	69.149	21.086	66.146
8	B-22-552-1, *Ap*	8.86	8.13	97.7	48.608	18.948	54.526
9	B-22-552-1, *Pl*	11.2	0.013	0.0679	15.446 (15.424)	15.214 (15.212)	35.056

Pb and U contents are given in ppm for apatite sample, and in ng in weighing bottle for stepwise leaching fractions. In the intervals between dissolution steps, the residue was not weighed in order to avoid the loss of apatite or its pollution. Lines 5–7 demonstrate the results of isotopic analysis of different (L2–L4) apatite fractions obtained by stepwise leaching. Lead isotopic data on plagioclase B-22-552-1 include measured values, as well as values corrected for fractionation, for total blank (without parentheses), and for uranium decay for an age of 1790 Ma (in parentheses).

Table 2. Results of Rb–Sr isotope studies of amphiboles and biotite from the metamorphosed sedimentary sequences of the Ladoga and Sortavala groups intruded by the gabbros of the Velimyaki massif

Rock name, number	Fraction	Rb	Sr	$^{87}Rb/^{86}Sr$	$^{87}Sr/^{86}Sr$	±2s	Model age, Ma
Two-mica gneiss, B3025	*Pl*	0.85	616	0.0040	0.717761	19	1717 ± 17
	Bt	288	3.50	548.7	14.036376	22	
Two-mica gneiss, B3024	WR	59.5	75.5	2.292	0.769219	10	1764 ± 17
	Bt	321.69	3.25	949.14	24.3898	24	
amphibolite, Б05-181	WR	26.1	136.5	0.5538	0.720126	4	1747 ± 11
	Amp	18.77	17.08	2.96	0.780566	5	
Amphibolite, Б05-183	WR	10.06	215.1	0.1357	0.708741	3	1729 ± 21
	Amp	9.52	25.43	1.082	0.732275	4	

(WR) whole rock. Measurement error is given in the last digit. Model age was calculated from the whole-rock–mineral pair (for sample B3025 – plagioclase–mineral).

To estimate the crystallization temperature of magmatic minerals, we used the chemical compositions of weakly altered pyroxenites (samples B-22-537-2 and B-22-550) that retained the intrusive textural and structural features and minerals of magmatic stage. Using COMAGMAT software, the liquidus temperatures were calculated for primary minerals of pyroxenites: 1264–1239°C for pyroxenes and 1220–1182°C for magnetites (Table 3). Ilmenite from these pyroxenites yielded slightly lower temperature of 954–920°C (Table 3).

The metamorphic stage of the Velimyaki massif is marked by the newly formed minerals, including hornblende, plagioclase, and biotite. Crystallization and recrystallization temperatures determined from the compositions of hornblende–plagioclase pairs using corresponding thermometer (Holland, Blundy, 1994), with some exception, fall within a range of 600–700°C (Table 4).

The lower temperature transformations identified due to the appearance of ilmenite and titanite are difficult to estimate quantitatively because of the absence of reliable mineral thermobarometers and probable disequilibrium state of these minerals at low temperatures. However, they likely occurred at temperature decrease up to 400–300°C based on the estimates from

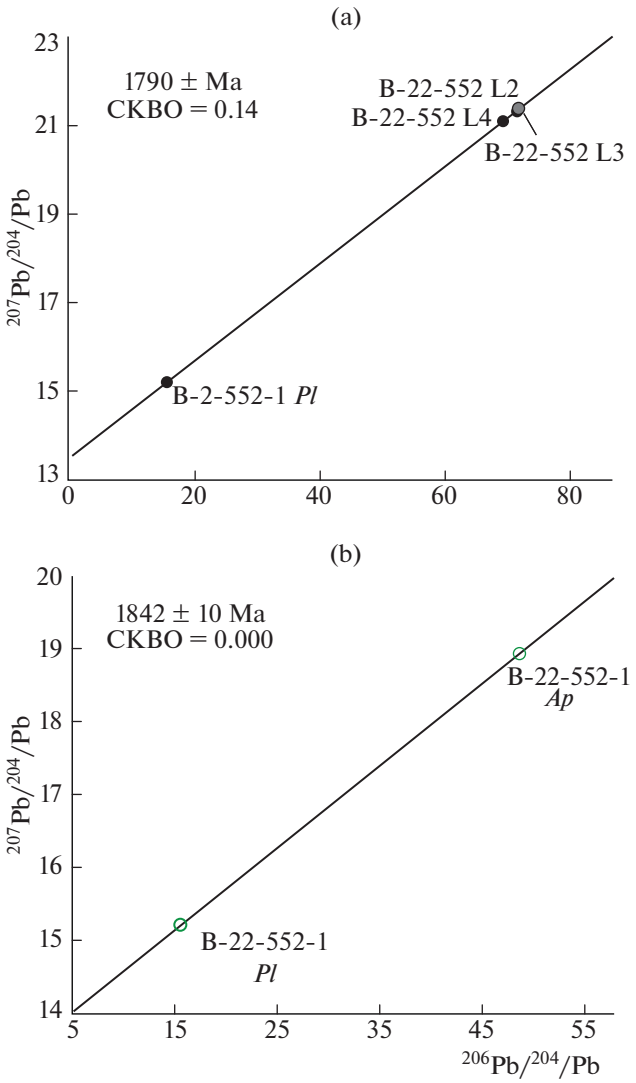

Fig. 8. Pb–Pb isochron for clinopyroxenite and monzogabbro from the Velimyaki massif, which were collected from one exposure. (a) Pb–Pb four-point isochron for apatite subjected to stepwise leaching (sample B-22-552, pyroxenite). Diagrams were plotted using the unradiogenic lead isotope composition of rock and the lead isotope compositions of apatite in leachates L2–L4, (b) Pb–Pb two-point isochron for apatite and plagioclase (sample B-22-552-1, monzogabbro).

Table 3. Thermometry using equilibrium equations in the systems "melt–pyroxene", "melt–magnetite" from a COMAGMAT software (Ariskin and Barmina, 2004)

Mineral	*P*, kbar	Sample	*T*, °C	Sample	*T*, °C
Aug	4-5	537-2	1264	550	1239
Mt	4-5	537-2	1182	550	1220
Ilm	4-5	537-2	920	550	954

Sample numbers are listed in table without prefix "B-22".

magnetite–ilmenite thermometer (Lepage, 2003). This temperature regime corresponds to the green schist facies metamorphism.

Based on the estimates from Ti-in-*Bt* thermometers (Henry et al., 2005; Wu and Chen, 2015), the (re)crystallization of biotite in equilibrium with ilmenite occurred at *T* around 490–620°C (using compositions of biotite from sample B-22-552-1). However, since this thermometer was not calibrated for basic composition, these temperatures are taken only as approximate. In general, it is suggested that the release of titanium from biotite and its reprecipitation as titanite with simultaneous formation of higher Fe biotite occurred within a temperature range from 700–600°C to 400–300°C.

The pressure of the magmatic stage of mineral formation was not determined by direct calculation with the use of magmatic minerals. It likely was close to the pressure in host rocks at the moment of magma chamber formation, which, judging from the barometry of metamorphic rocks, accounted for around 4–5 kbar (Baltybaev et al., 2000).

Pressure estimates using hornblende–plagioclase barometer (Molina et al., 2015) yield 4–7 kbar for the metamorphic stage of gabbro recrystallization (Table 4) at accepted equilibrium temperature for these two minerals within 600–700°C.

DISCUSSION

The observed recrystallization of postmagmatic minerals of gabbros of the studied massif is reflected in the textural-structural features of rocks, a change of mineral assemblages and chemical compositions of minerals. The revealed transformations are related to the regional metamorphic processes, which, judging from obtained data, caused the recrystallization of ore minerals and apatite. The overall postmagmatic alterations first of all caused the development of secondary minerals after pyroxenites and gabbros in form of amphibolization and biotitization of clinopyroxene.

The first stage of amphibolization is expressed in the development of actinolite after clinopyroxene as rims or full pseudomorphs. Simultaneously, titanite forms rims around titanomagnetite grains or separate grains within biotite aggregates. Changes of biotite that are accompanied by the formation of titanite are characterized by an increase of its Fe mole fraction and decrease of Ti content.

Subsequent replacement of actinolite by hornblende in association with moderate-Ca plagioclase was caused by a change of mineral formation conditions. Judging from *PT*-estimates, this was related to the temperature increase up to the amphibolite facies. The fact that regional metamorphism also corresponds to this facies points to the isofacies conditions of the hornblende–plagioclase paragenesis in the

Table 4. Mineral thermobarometry of the metamorphic stage of gabbroids of the Velimyaki massif

Phase	Sample	*Hbl*, No.	Morphology	*Pl*, No.	*T*, °C		*P*, kbar	
					1 kbarp	5 kbar	600°C	700°C
1	552-1	14	Grain	10	707	732	–	–
		46	Rim	45	629	661	–	–
		47	Grain	45	617	647	–	–
		66	Grain	68	645	675	5	7
		67	Rim	68	657	690	–	–
		74	Grain	81	655	692	–	–
		80	Grain	78	707	740	5	7
		103	Rim	102	665	694	–	–
		108	Grain	109	715	744	4	7
		110	Grain	111	626	663	–	–
		134	Grain	135	608	647	–	–
		136	Grain	137	615	644	–	–
		138	Grain	139	677	704	4	7
2	541	50	Grain	52	735	772	–	–
		76	Grain	78	734	769	–	–
		95	Grain	96	642	699	–	–
		120	Grain	122	620	682	–	–
	544	39	Rim	41	684	707	–	–
		63	Rim	65	725	755	–	–
		67	Rim	73	730	750	–	–
		103	Rim	104	676	710	–	–
		113	Rim	114	728	748	–	–

Temperatures were calculated after thermometer (Holland and Blundy, 1994), while pressure, after barometer (Molina et al., 2015). Sample numbers are listed in table without prefix "B-22".

metagabbrods of the Velimyaki massif and mineral parageneses of surrounding metamorphic rocks.

The lowest temperature changes of metagabbros involve the formation of carbonate in the interstices and epidotization of clinopyroxene, amphiboles, and, partly, biotite.

Thus, the above mentioned change of mineral associations in the metagabbros of the studied massif indicates a long-term postmagmatic stage under *PT*-conditions of amphibolite metamorphic facies and subsequent lower temperature facies. The fact that apatite grains in the metamorphosed pyroxenites, monzogabbro, and monzodiorites are confined to the newly formed hornblende, plagioclase, and biotite indicate its relation with postmagmatic stage. This is also consistent with obtained Pb–Pb apatite age (1.84–1.79 Ga), which points to a significant time gap between magmatic and metamorphic stages of rock formation. However, the question arises whether the younger age of apatite record the time of U–Pb system closure in it at rock cooling or the recrystallization/new formation of this mineral?

Judging from numerous literature data (Kärkkäinen and Appelqvis, 1999; Cochrane et al., 2014; Kirkland et al., 2018; O'Sullivan et al., 2020; Chew and Spikings, 2021, and others), both variants are possible in natural objects depending on the definite conditions of mineral formation, such as tectonic and temperature regime of petro- and ore genesis, cooling rate, and other factors.

The papers (Cochrane et al., 2014; Chew and Spikings, 2021) test the key point of thermochronology on the thermally activated volume diffusion of isotopes from crystals. An alternative mechanism to the volume diffusion could be the transport of isotopes with the predominant effect of fluid percolation in grains along fractures, lattice defects, and others. A revealed positive correlation between grain size and its U–Pb age in combination with consistent temperature–time curves obtained by ID-TIMS and LA-MC-ICP-MS methods made it possible to suggest that Pb from apatites was lost owing to the thermally activated diffusion. By the similar manner, Paul et al. (2019) compared the application of bulk (ID-TIMS) and local (LA-MC-ICP-MS) dating methods for the recovery

of the thermal history of rocks from apatite that partially lost Pb.

However, the U–Pb age of apatite not always reflects the stage of cooling and closure of isotope system in the rock. For instance, using the rocks of the Akia terrane (Greenland) as an example, Kirkland et al. (2018) demonstrated that rims in the apatite grains were formed owing to the recrystallization, dissolution, and repeated growth of this mineral at temperature below the temperature of possible Pb diffusion in apatite (375–600°C). This indicates that apatite will not necessarily be characterized by the diffusion losses of Pb. To determine the cooling history, it is required to substantiate the applicability of mechanism of thermally activated volume diffusion. It was noted in the paper that the chemical and age zoning in apatite grains cannot coincide due to the different diffusion rates of trace elements, in particular, U and Pb.

Conclusion concerning the late crystallization of apatite was also made at studying the Kiglapait intrusion (Canada), which hosts massive Ti-bearing magnetite horizons. It was established that its titanomagnetite horizons were accumulated already after 93–94% crystallization of the intrusion and apatite has begun to crystallize only by that time (Morse, 1980). By the similar manner, it was suggested that apatite in the Skaergaard intrusion (Greenland) has begun to precipitate after 97% crystallization of the intrusion and the remained magma contained 1.75% P_2O_5 content (Raierson and Hess, 1980). Magmatic genesis is suggested for the apatite–magnetite ores of the Northern Gurvunur deposit in Western Transbaikalia (Ripp et al., 2017), the homogenous oxygen isotope composition of which throughout the entire section of ore lode is explained by the relation with a mantle source, while the temperature of oxygen isotope equilibrium of 620–800°C for the apatite–magnetite pair is interpreted as supporting the magmatic origin of the ores.

The studied gabbroids of the Velimyaki massif were subjected to the intense Paleoproterozoic metamorphism, which spanned the rocks in the junction zone of the Svecofennian belt and the southern margin of the Karelian craton. The oldest metamorphic monazites have an U–Pb ID-TIMS age of 1878–1874 Ma (Baltybaev et al., 2009, 2024). However, there are also the younger metamorphic monazites, whose U–Pb ID-TIMS ages point to the repeated thermal events at 1794–1786 Ma (Baltybaev et al., 2009, 2024). Correspondingly, the monazites of two age groups are correlated with Early and Late Svecofennian metamorphic events in the region at ~1.88 and ~1.80 Ga. The age of the older monazite coincides with the U–Pb SIMS age of zircon (1876 ± 12 Ma) from migmatite leucosomes in the vicinity of gabbroid massifs, but these zircons have metamorphic rims with an age of 1805 ± 18 Ma (Baltybaev et al., 2009). The age of these rims within error coincides with the age of most metamorphic monazites of this region (1.80–1.79 Ga), with Rb–Sr model ages of amphibole and biotite (Table 2), and corresponds to the timing of Late Svecofennian tectonothermal activity on the southern margin of the Karelian Craton.

Note that the Late Svecofennian metamorphism identified from Sm–Nd isotope data on amphiboles, titanite, and plagioclase revealed the beginning of the Late Scecofennian metamorphic stage in the region within 1.84–1.83 Ga (Baltybaev et al., 2024). Such age values are close to the older age estimates on apatites obtained in this work.

Thus, the Velimyaki massif is located in the region, where tectonothermal activation occurred in two stages: ~1.88 and ~1.80 Ga. The regional character of near-cratonic endogenous activation also follows from isotope dates of titanite in the junction zone of the Karelian Craton and rocks of the Belomorian mobile belt, which also revealed the fluid-thermal reworking of rocks at 1.80–1.75 Ga (Bibikova et al., 1999, 2004).

A large time gap of apatite age from the age of magmatic zircon from the Velimyaki massif and the coincidence of the former with active metamorphic events in the region rather points to the complete metamorphic recrystallization of the apatite. One of the geochemical criteria of postmagmatic formation of apatite could be the absence of any differences in the contents of volatile components in apatite from rocks of the first and second phases (Fig. 6), although the study of apatite compositions, for instance in (Romanchev, 1990; Savko et al., 2007; Barkov et al., 2021) reveals their variability during evolution of fractionating melt.

The apatite recrystallization is supported by the presence of inclusions of REE-bearing minerals (monazite, xenotime, and allanite), formation of which could be related to the REE release into the own phase during metasomatism or metamorphism (Harlov, 2015). The presence of allanite inclusions in apatite grains or on the contacts of apatite grains with other minerals in the rocks of the Velimyaki massif could additionally indicate that apatite mineralization is newly formed (Fig. 9).

The attention should be focused on the relationship of titanomagnetite ores with enrichment of rocks in phosphorus. For instance, layered mafic intrusions (Morse, 1980, 1990; Lee, 1996), including some Svecofennian differentiated intrusive bodies (for instance, see Makinen, 1987; Makkonen, 1996, and others), are formed through fractional crystallization with simultaneous magma enrichment in phosphorus and iron. The simultaneous enrichment in titanium and phosphorus was noted in rocks of the Kuhajarvi intrusion in Eastern Finland (Kärkkäinen and Appelqvis, 1999). The simultaneous enrichment in apatite, ilmenite, and magnetite could be exemplified by zones in the upper gabbroic sequence of the Bushveld Complex (Reynolds, 1985a, 1985b; von Gruenewaldt, 1993).

The enrichment in titanium and phosphorus in rocks of the Kuhajariv intrusion is thought to be related

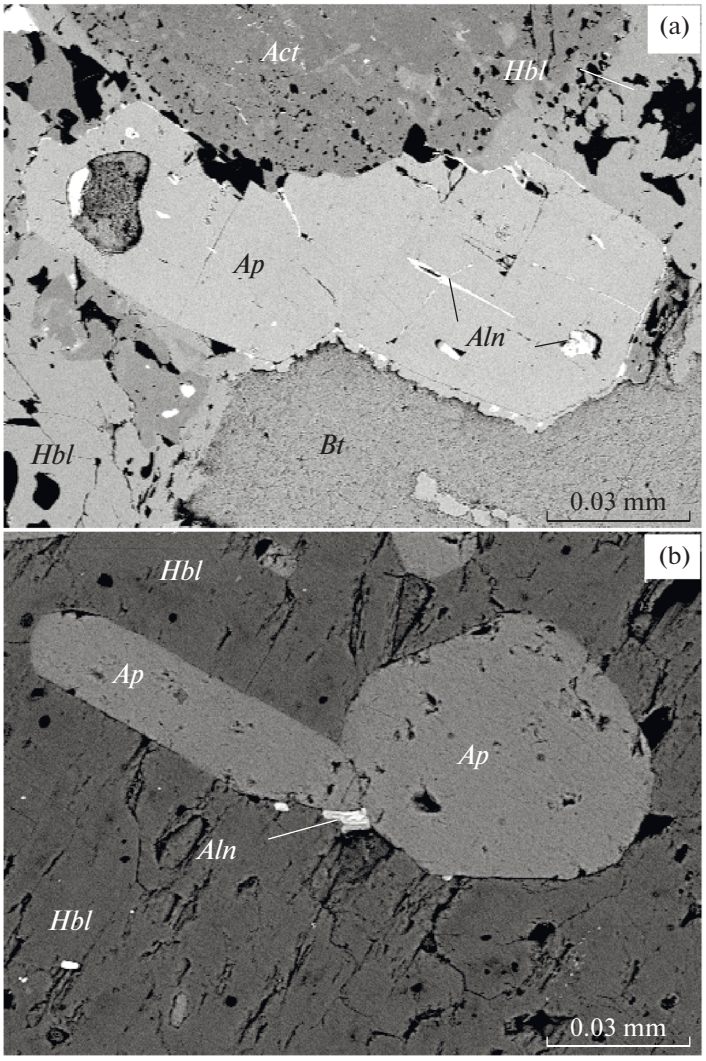

Fig. 9. BSE images of apatite grains in association with allanite from rocks of the Velimyaki massif (samples B-22-552-1, B-22-541). (a) exsolution (?) of REE apatite at recrystallization of apatite, (b) allanite in contact with apatite grains in a hornblende matrix

to the mixing of tholeiitic and granite magmas at the late stage of Svecofennian orogeny or, likely, after it. It is suggested that magma mixing led to the increase of F, P, and Ti contents in the tholeiitic magma (Kärkkäinen and Appelqvis, 1999). This is consistent with experimental studies of Watson (Watson, 1976), who demonstrated that phosphorus and titanium in the bimodal felsic—basic system are mainly partitioned into basic magma. This is also confirmed by the fact that the titanium solubility in the tholeiitic magma increases with the growth of phosphorus content (e.g., Ryerson and Hess, 1980). Fluorine in the basic magma of the Kuhajarvi intrusion is considered to be of crustal origin, because this element strongly enriches host schists (Wedepohl, 1970).

The considered apatite-bearing ores of the Velimyaki massif also show evidence for the crustal contamination. K-feldspars from this intrusion (Baltybaev et al., 2017) have high $\mu = 10.4–10.8$ corresponding to the upper crustal characteristics. It was also revealed that the latest sulfide- and gold-bearing hydrothermal-metasomatic veins in the gabbroids were formed during Caledonian tectogenesis within 400–460 Ma (Baltybaev et al., 2017, 2020). Crustal contamination of mantle magmas could be responsible for the elevated potassium contents in the Velimyaki magma, which determined the unusual subalkaline trend of the gabbroids. Additional isotope-geochemical studies are required to solve some questions including the following: (a) whether postmagmatic apatites in the gabbroids were formed in several stages; (b) whether magma source was isotopically and geochemically homogenous and whether the Pb isotopic compositions of low-uranium minerals retained the isotopic characteristics of initial lead.

CONCLUSIONS

Ore apatite-bearing mineralization in the gabbroids of the Velimyaki massif was formed through several stages. Magmatic stage was responsible for the formation of early rock-forming mineral assemblages and accumulation of apatite-bearing titanomagnetite ores through the crystallization from a magmatic melt.

The titanomagnetite ores and associated apatite experienced recrystallization at the postmagatic and especially metamorphic stages, which significantly affected the U–Pb system of apatite, leading to resetting of this isotope system. Isotopic Pb–Pb ages of apatite indicate a large time gap between the re-equilibration of U–Pb system and the stage of magmatic crystallization of primary rock-forming minerals in the ore clinopyroxenites and gabbro. This time coincides with the Late Svecofennian (with peak at 1.81–1.79 Ga) multiple stage of regional metamorphism, which spanned also the rocks of the Velimyaki massif.

PT-parameters of the Late Svecofennian metamorphic reworking of gabbroids of the studied massif correspond to the amphibolite metamorphic facies with further decrease to the greenschist facies. The latest fluid-thermal events also spanned the rocks of the Velimyaki massif in the Phanerozoic and were expressed in the formation of hydrothermal-metasomatic veins along local thin tectonic zones.

SUPPLEMENTARY INFORMATION

The online version contains supplementary material available at https://doi.org/10.1134/S0016702924700654.

ACKNOWLEDGMENTS

We are grateful to Yu. O. Larionava (IGEM, Moscow) and anonymous reviewer who revised the first version of the manuscript and gave very useful recommendations to improve it. We are also grateful to the scientific editor, Yu. A. Kostitsyn, for organization and preparation of this paper.

FUNDING

This work was made in the framework of government-financed task of the Institute of Precambrian Geology and Geochronology, project no. FMUW-2022-0002.

CONFLICT OF INTEREST

The authors of this work declare that they have no conflicts of interest.

REFERENCES

I. A. Alekseev and L. V. Kuleshevich, "Noble-metal mineralization of Vyalimäki massif (Northern Ladoga region, Karelia)," Trudy KarNTs RAN. Geologiya dokembriya **2**, 60–72 (2017).

I. A. Alekseev, "Noble-metal mineralization of Vyalimäki massif (Northern Ladoga region)," *Proceedings of the XVI Youth Conf. in Memory of K. O. Kratz,* (Petrozavodsk, 2005), pp. 244–247

I. A. Alekseev, I. K. Kotova, and S. V. Petrov, "Gold ore occurrence in Vyalimäki massif (Northern Ladoga region)," Vestn. SPbGU **7** (3), 107–110 (2005).

A. A. Ariskin and G. S. Barmina, *Modeling of Phase Equilibria during Crystallization of Basaltic Magmas* (Nauka, Moscow, 2000).

A. A. Ariskin and G. S. Barmina, "COMAGMAT: Development of a magma crystallization model and its petrological applications," Geochem. Int **4** (1), 1–157 (2004).

Sh. K. Baltybaev, V. A. Glebovitsky, I. V. Kozyreva, D. L. Konopel'ko, O. A. Levchenkov, I. S. Sedova, and V. I. Shul'diner, *Geology and Petrology of the Ladoga Region*, Ed. by V. A. Glebovitsky (SPbGU, 2000).

Sh. K. Baltybaev, O. A. Levchenkov, V. A. Glebovitsky, L. K. Levskii, A. F. Makeev, and S. Z. Yakovleva, "Polychronous nature of metamorphic zoning: evidence from U–Pb and Pb–Pb dating of metamorphic rocks (Southern Karelia, Baltic Shield), " Dokl. Earth Sci. **401A** (4), 361–363 (2005).

Sh. K. Baltybaev, O. A. Levchenkov, V. A. Glebovitsky, et al., "Early migmatites in the prograde metamorphism zone of gneisses in the northern domain of the Ladoga Region: U–Pb evidence based on monazite," Dokl. Earth Sci. **420** (4), 589–591 (2008).

Sh. K. Baltybaev, A. N. Larionov, O. A. Levchenkov, et al., "U–Pb geochronology of migmatite leucosomes based on zircon SIMS measurements and correlation with TIMS-ID data on monazite," Dokl. Earth Sci. **427** (6), 943–946 (2009).

Sh. K. Baltybaev, G. V. Ovchinnikova, V. A. Glebovitskii, et al., "Caledonian formation of gold-bearing sulfide depositions in Early Proterozoic Gabbroids in the northern Ladoga Region," Dokl. Earth Sci. **476** (2), 992–996 (2017).

Sh. K. Baltybaev, G. V. Ovchinnikova, A. B. Kuznetsov, I. M. Vasil'eva, N. G. Rizvanova, I. A. Alekseev, and P. A. Kirillova, "Two stages of gold-sulfide mineralization in early Proterozoic gabbroids of the Northern Ladoga region," Vestn. SPbGU. Nauki o Zemle **66** (3), 559–577 (2020).

Sh. K. Baltybaev, V. M. Savatenkov, and M. E. Petrakova, "T-t evolution of Early Proterozoic rocks of the Northern Ladoga region according to the study of U–Pb, Pb–Cr and Sm–Nd systems in minerals," Geodynam. Tectonophys. **15** (3) (2024). https://doi.org/10.5800/GT-2024-15-3-0759

A. Yu. Barkov, E. V. Sharkov, A. A. Nikiforov, V. N. Korolyuk, and S. A. Sil'yanov, "Compositional variations of apatite and REE-Bearing minerals in relation to crystallization trends in the Monchepluton Layered Complex (Kola Peninsula)," Russ. Geol. Geophys. **62** (4), 427–444 (2021).

E. V. Bibikova, A. I. Slabunov, S. V. Bogdanova, T. Skiöld, V. S. Stepanov, and E. Yu. Borisova, "Early magmatism of the Belomorian Mobile Belt, Baltic Shield: lateral zoning and isotopic age," Petrology **7** (2), 123–146 (1999).

E. V. Bibikova, S. V. Bogdanova, V. A. Glebovitsky, S. Claesson, and T. Skiöld, "Evolution of the Belomorian Belt: NORDSIM U-Pb zircon dating of the Chupa paragneisses, magmatism, and metamorphic stages," Petrology **12** (3), 227–244 (2004).

D. M. Chew and R. A. Spikings, "Apatite U-Pb thermochronology: a review," Minerals **11** (10), 1095 (1095). https://doi.org/10.3390/min11101095

R. Cochrane, R. A. Spikings, D. Chew, J.-F. Wotzlaw, M. Chiaradia, Sh. Tyrrell, U. Schaltegger, and R. Van Der Lelij, "High temperature (>350°C) thermochronology and mechanisms of Pb loss in apatite," Geochim. Cosmochim. Acta **127**, 39–56 (2014). https://doi.org/10.1016/j.gca.2013.11.028

Z. T. Gromova, *Report of the South Karelian Expedition on Prospecting and Exploration Works to Reveal the Nature of the Velimyaki Magnetic Anomaly* (Fondy KGE, Petrozavodsk, 1951).

D. E. Harlov, "Apatite: a fingerprint for metasomatic processes," Elements **11** (3), 171–176 (2015). https://doi.org/10.2113/gselements.11.3.171

D. J. Henry, C. V. Guidotti, and J. A. Thomson, "The Ti-saturation surface for low-to-medium pressure metapelitic biotites: Implications for geothermometry and Ti-substitution mechanisms," Am. Mineral. **90** (2-3), 316–328 (2005). https://doi.org/10.2138/am.2005.1498

T. Holland and J. Blundy, "Non-ideal interactions in calcic amphiboles and their bearing on amphibole-plagioclase thermometry," Contrib. Mineral. Petrol. **116** (4), 433–447 (1994). https://doi.org/10.1007/bf00310910

V. I. Ivashchenko and A. I. Golubev, *Gold and Platinum of Karelia: Formation-Genetic Types of Mineralization and Prospects* (KarNTs RAN, Petrozavodsk, 2011).

V. I. Ivashchenko and O. B. Lavrov, "Noble-metal mineralization of Southwestern Karelia," in *Problems of Gold and Diamondiferous Mineralization in the North of the European Part of Russia*, Ed. by A. I. Golubev and S. I. Rybakov (KarNTs RAN, Petrozavodsk, 1997), pp. 44–51.

R. A. Khazov, M. G. Popov, and N. S. Biske, *Riphean Potassic Alkaline Magmatism of the Southern Part of the Baltic Shield* (St. Petersburg, 1993).

C. L. Kirkland, C. Yakymchuk, K. Szilas, N. Evans, J. Hollis, B. Mcdonald, and N. J. Gardiner, "Apatite: a U-Pb thermochronometer or geochronometer?," Lithos **318–319**, 143–157 (2018). https://doi.org/10.1016/j.lithos.2018.08.007

N. Kärkkäinen and H. Appelqvist, "Genesis of a low-grade apatite-ilmenite-magnetite deposit in the Kauhajärvi gabbro, western Finland," Mineral. Deposita **34** (8), 754–769 (1999). https://doi.org/10.1007/s001260050236

Ladoga Proterozoic Structure (Geology, Deep Structure, and Mineralogy), Ed. by N. V. Sharov (Karel'skii nauchnyi tsentr RAN, Petrozavodsk, 2020).

C. A. Lee, "A review of mineralization in the Bushveld Complex and some other layered intrusions," in *Developments in Petrology*, Ed. by R. G. Cawhorn (Elsevier, Amsterdam, 1996), pp. 103–145. https://doi.org/10.1016/s0167-2894(96)80006-6

L. D. Lepage, "ILMAT: an Excel worksheet for ilmenite–magnetite geothermometry and geobarometry," Comp. Geosci. **29** (5), 673–678 (2003). https://doi.org/10.1016/s0098-3004(03)00042-6

S. B. Lobach-Zhuchenko, V. P. Chekulaev, and V. S. Baikova, *Precambrian Epochs and Types of Granite Formation in the Baltic Shield* (Leningrad, 1974).

A. J. Locock, "An Excel spreadsheet to classify chemical analyses of amphiboles following the IMA 2012 recommendations," Comput. Geosci. **62**, 1–11 (2014). https://doi.org/10.1016/j.cageo.2013.09.011

K. R. Ludwig, "User's manual for Isoplot/Ex, version 3.00, a geochronological toolkit for Microsoft Excel," Berkeley Geochronology Center. Spec. Publ. **4**, (2003).

J. Makinen, "Geochemical characteristics of Svecokarelidic mafic-ultramafic intrusions associated with Ni–Cu occurrence in Finland," Geol. Surv. Finland Bull **342**, (1987).

H. Makkonen, "1.9 Ga tholeiitic magmatism and related Ni–Cu deposits in the Juva area.SE Finland," Geol. Surv. Finland Bull **386**, (1996).

G. Manhes, J. F. Minster, and C. J. Allègre, "Comparative uranium-thorium-lead and rubidium-strontium study of the Saint Sèverin amphoterite: consequences for early solar system chronology," Earth Planet. Sci. Lett. **39** (1), 14–24 (1978). https://doi.org/10.1016/0012-821x(78)90137-1

Mineral Raw Base of the Republic of Karelia, Ed. by V. P. Mikhailov and V. N. Aminov (Petrozavodsk, 2005).

J. F. Molina, J. A. Moreno, A. Castro, C. Rodríguez, and G. B. Fershtater, "Calcic amphibole thermobarometry in metamorphic and igneous rocks: New calibrations based on plagioclase/amphibole Al-Si partitioning and amphibole/liquid Mg partitioning," Lithos **232**, 286–305 (2015). https://doi.org/10.1016/j.lithos.2015.06.027

S. A. Morse, "Kiglapait mineralogy II: Fe-Ti oxide minerals and the activities of oxygen and silica," J. Petrol. **21** (4), 685–719 (1980). https://doi.org/10.1093/petrology/21.4.685

S. A. Morse, "The differentiation of the Skaergaard intrusion. Discussion of Hunter and Sparks," Contrib Mineral Petrol **95**, 451–461 (1990).

G. O'Sullivan, D. Chew, G. Kenny, I. Henrichs, and D. Mulligan, "The trace element composition of apatite and its application to detrital provenance studies," Earth-Sci. Rev. **201**, 103044 (2020). https://doi.org/10.1016/j.earscirev.2019.103044

A. N. Paul, R. A. Spikings, D. Chew, and J. S. Daly, "The effect of intra-crystal uranium zonation on apatite U-Pb thermochronology: A combined ID-TIMS and LA-MC-ICP-MS study," Geochim. Cosmochim. Acta **251**, 15–35 (2019). https://doi.org/10.1016/j.gca.2019.02.013

I. M. Reynolds, "Contrasted mineralogy and textural relationships in the uppermost titaniferous magnetite layers of the Bushveld Complex in the Bierkraal area north of Rustenburg," Econ. Geol. **80** (4), 1027–1048 (1985). https://doi.org/10.2113/gsecongeo.80.4.1027

I. M. Reynolds, "The nature and origin of titaniferous magnetite-rich layers in the upper zone of the Bushveld Complex; a review and synthesis," Econ. Geol. **80** (4),

1089–1108 (1985).
https://doi.org/10.2113/gsecongeo.80.4.1089

G. S. Ripp, E. V. Khodyreva, I. A. Izbrodin, M. O. Rampilov, E. I. Lastochkin, and V. F. Posokhov, "Genetic nature of apatite–magnetite ore in the north Gurvunur Deposit, Western Transbaikal Region," Geol. Ore Deposits **59** (5), 407–420 (2017).

B. P. Romanchev and V. L. Bocharov, "Genetic types of apatite from the Dubravinsky massif of KMA," Geokhimiya **7**, 1047–1052 (1990).

F. J. Ryerson and P. C. Hess, "The role of P_2O_5 in silicate melts," Geochim. Cosmochim. Acta **44** (4), 611–624 (1980).
https://doi.org/10.1016/0016-7037(80)90253-7

G. M. Saranchina, "Petrology of the Velimyak intrusion and associated ore occurrence," Izv. Karelo-Finsk. Nauchn.-Issled. Bazy AN SSSR **2**, 32–42 (1948).

V. M. Savatenkov, I. M. Morozova, and L. K. Levsky, "Behavior of the Sm-Nd, Rb-Sr, K-Ar, and U-Pb isotopic systems during alkaline metasomatism: fenites in the outer-contact zone of an ultramafic-alkaline intrusion," Geochem. Int **42** (10), 899–920 (2004).

K. A. Savko, S. M. Pilyugin, and M. A. Novikova, "Apatite composition from rocks of different-age ferruginous-siliceous formations of the Voronezh crystalline massif - as an indicator of the fluid regime of metamorphism," Vestn. VGU, Seriya: Geol., No. 2, 78–91 (2007).

N. G. Sudovikov, V. A. Glebovitsky, A. S. Sergeev, et al., *Geological Development of Deep Zones of Mobile Belts (Northern Ladoga Region)* (Nauka, Leningrad, 1970), Vol. 227.

P. Vermeesch, "IsoplotR: A free and open toolbox for geochronology," Geosci. Front. **9** (5), 1479–1493 (2018).
https://doi.org/10.1016/j.gsf.2018.04.001

G. Von Gruenewaldt, "Ilmenite–apatite enrichments in the upper zone of the Bushveld Complex: a major titanium–rock phosphate resource," Int. Geol. Rev. **35** (11), 987–1000 (1993).
https://doi.org/10.1080/00206819309465570

E. B. Watson, "Two-liquid partition coefficients: Experimental data and geochemical implications," Contrib. Mineral. Petrol. **56** (1), 119–134 (1976).
https://doi.org/10.1007/bf00375424

K. H. Wederpohl, *Handbook of Geochemistry* (Springer, Berlin-Heidenderg-New York, 1970).

D. L. Whitney and B. W. Evans, "Abbreviations for names of rock-forming minerals," Am. Mineral. **95** (1), 185–187 (2010).
https://doi.org/10.2138/am.2010.3371

C.-M. Wu and H.-X. Chen, "Revised Ti-in-biotite geothermometer for ilmenite- or rutile-bearing crustal metapelites," Sci. Bull. **60** (1), 116–121 (2015).
https://doi.org/10.1007/s11434-014-0674-y

Translated by M. Bogina

SPELL: OK